Sensors and Materials, Vol. 36, No. 2 (2024) 767–777
MYU Tokyo

S & M 3560

Development of Smartphone-based Detection for *Helicobacter pylori* Rapid Test

Yu-Lin Wu,[1] Wei-Chien Weng,[1] Yi-Hsuan Chen,[1] and Yu-Cheng Lin[1,2*]

[1]Department of Engineering Science, National Cheng Kung University,
No. 1, University Road, Tainan City 70101, Taiwan
[2]Institute of Innovative Semiconductor Manufacturing, National Sun Yat-sen University,
No. 70 Lien-hai Road, Kaohsiung City 804201, Taiwan

(Received September 16, 2023; accepted February 13, 2024)

Keywords: HPY, HpSA, rapid test, image processing, ArUco marker, color calibration, perspective transformation

Helicobacter pylori (HPY) is a type of spiral bacterium. The International Agency for Research on Cancer (IARC) has classified HPY as a Group 1 carcinogen, indicating that it is the leading cause of stomach cancer. The traditional testing method for HPY is cumbersome and requires professional personnel to operate. Owing to advances in biochemical technology, rapid tests for HPY have been developed. The development of the rapid test is based on colloidal gold. The rapid test displays two lines when the result is positive. The color of the test result can vary due to changes in the size or concentration of colloidal particles. Users may misinterpret the results owing to the effect of ambient lighting or when the color is too close to the background color. In this study, we successfully developed a method for using a smartphone to evaluate the results and sample concentration in rapid tests for detecting HPY. The HPY rapid test is placed on a colorimetric board developed for this study, and an image is captured using a smartphone and evaluated using the image processing program designed in this research. The ArUco marker is used for positioning and color correction to ensure that it is not affected by the brand of the camera of the mobile phone and nonuniform ambient light sources. To confirm whether the proposed method correctly determines the result and sample concentration, experiments were conducted using multiple different mobile phones. In the experiment, the illumination and shooting height were fixed and several different sample concentrations were used. Printed simulated and real rapid test results were used in the experiment. The experimental results show that both positive and negative can be correctly determined, and there is good linearity when determining each concentration of samples from the image. For example, when using simulated rapid tests, the R^2 value is at least 0.9915, and the detection concentration threshold of the real HPY rapid tests is 5000 CFU/mL. Even with the concentration at 1250 CFU/mL, the R^2 value is still 0.9473.

*Corresponding author: e-mail: yuclin@mail.ncku.edu.tw
https://doi.org/10.18494/SAM4798

ISSN 0914-4935 © MYU K.K.

1. Introduction

Helicobacter pylori (HPY) is a type of spiral bacterium that can survive in the stomach and duodenum. Most infected people may have gastric mucosal inflammation or gastritis, and some people may develop gastric ulcers, other gastrointestinal diseases, and even gastric cancer. The International Agency for Research on Cancer (IARC) has classified HPY as a Group 1 carcinogen.[1] With the outbreak of COVID-19 in 2020, rapid tests have become a familiar daily necessity. The advantage of rapid tests is that users can undergo the test rapidly and instantly confirm the cause and condition, which will facilitate subsequent treatment. Common rapid test items include COVID-19, pregnancy, and urine 10 items (URS-10).[2–4] The traditional HPY test methods are the rapid urease test (HUT) and 13C-urea breath test (13C-UBT).[5] In recent years, owing to the advancement of biochemical technology, the rapid test for HPY based on *Helicobacter pylori* Stool Antigen (HpSA) has been developed.[6] The rapid test developed based on colloidal gold displays two lines, namely, the control line (C line) and the test line (T line), if the result is positive. The accuracy is not less than that of traditional detection methods and is easy to identify. According to the research proposed by Rey *et al.* in 2017, the T line will change color in accordance with the concentration of the detection solution, which means that users may misjudge low concentration results owing to the effects of ambient lighting or their own ignorance of the rapid test characteristics.[7] Fortunately, machine vision is now widely used in industry for identification.[8] Using machines to identify the results of rapid tests can increase accuracy and enable timely treatment for users.

Applying machine vision for identification will cause many problems, such as the positioning of the detection target, the skew of the shooting target, and the influence of ambient light sources. The ArUco marker is a positioning marking system developed by Garrido-Jurado *et al.* and is usually used in augmented reality, robot positioning, and pose estimation.[9] It plays an indispensable role in the field of computer vision. The ArUco marker, which consists of a black rectangle and an internal binary matrix, is suitable for detection in this study. The black border facilitates quick detection of images. The binary encoding can be used in error detection and correction techniques. In addition, the internal matrix also represents a marker ID.

If the target is skewed in the image, it will be difficult to establish coordinates. This problem may exacerbate detection failure. Perspective transformation, also known as projection mapping, is a technology that projects images to a new visual plane. The skewed image in the three-dimensional space is mapped and converted to a new image plane. This process can solve the problem of difficult positioning of the image on the original image plane, which makes it difficult to establish coordinates. Perspective transformation is widely used in three-dimensional image processing. For example, in 2013, Do proposed the application of mapping conversion for image scaling.[10] Stamatopoulos *et al.* in 2011 also proposed the application of perspective transformation in images to solve the problem of file distortion caused by shooting angles.[11]

Under the influence of ambient light sources and cameras of different brands, the color captured may be different from the original color. For this reason, the image needs to be color calibrated.[12] Color calibration is also called color restoration, and there are many ways to achieve the corrections desired when using this technique. The first color calibration card

(ColorChecker) was issued by Macbeth in 1976, and it is now an indispensable form of technology in the photography, film, and television industries.[13]

Smartphones have become an indispensable part of people's lives, and related research on image recognition using smartphones has emerged one after another. Among them, as research related to the identification of the results of rapid tests, Cao *et al.* used red beet pigments that react with copper ions (Cu^{2+}) through a redox reaction to detect the concentration of Cu_2+ in drinking water and used smartphones to determine the concentration of Cu^{2+}.[14] In 2019, Phadungcharoena *et al.* established a linear relationship between blue channel of images and drug concentration based on the measurement of the color change of penicillamine and thiolate polymers using a smartphone and then used the reaction of the Ellman reagent to determine the concentration of penicillamine.[15] On the basis of the above method, we integrated a smartphone with several image processing technologies to identify the HPY test results and determine the sample concentration.

2. Materials and Methods

In this study, we used a smartphone to capture images of HPY rapid test results and to analyze them. The test images were taken by users. The result window in the pictures may have problems such as tilt, offset, uneven ambient light, and blur. To avoid affecting the detection of the results, we used a variety of methods to adjust the images, including perspective transformation and color correction, to overcome these problems. To implement the above methods, we divided the methodology in this study into two parts: hardware and image processing. In the hardware part, a colorimetric board was developed as an auxiliary correction method. The appearance of the board is shown in Fig. 1.

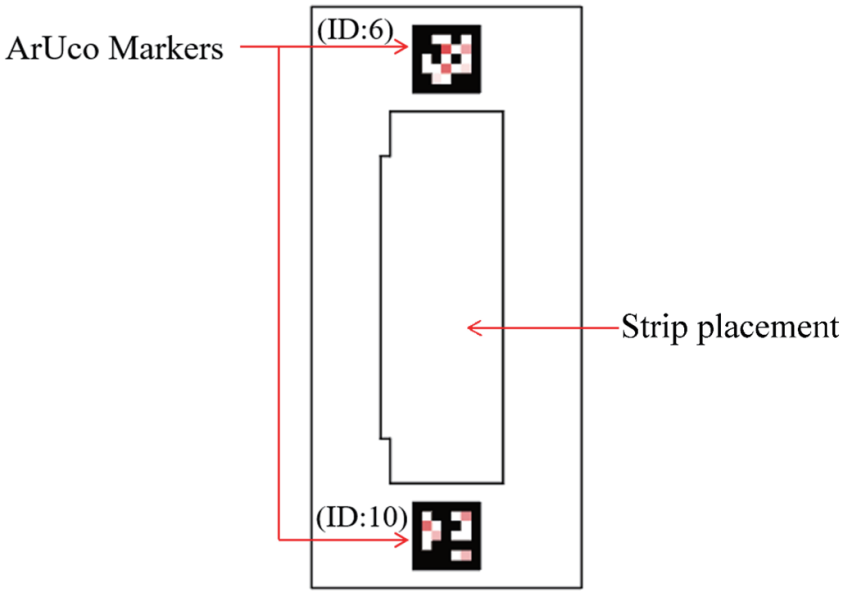

Fig. 1. (Color online) Colorimetric board used in this study.

The surface of the colorimetric board was printed with marks for alignment and color calibration. The colorimetric board has grooves for placing reagents. ArUco markers were used for positioning. We used perspective transformation to correct any angle tilt caused by the user during photography. This process puts the rapid test in the center of the image, making it easier to capture the position of the test result. To avoid the effect of the user's ambient light source or cameras of different brands on the interpretation of the results, the concept of color correction was applied in this study. To avoid environmental light sources or difference between camera brands affecting the interpretation of the results, the concept of color correction was applied. The color of the T line changes with the HPY concentration. The result is a single color, so it does not require color calibration for the whole picture. The method proposed in this study uses the color rendering of four different concentrations of reagents as a comparison target. To reduce the area of the colorimetric board, we replaced several black blocks at fixed positions in the internal binary matrix of the ArUco markers with correction color blocks. The ArUco markers used in this study are shown in Fig. 2.

The image processing part comprises the processing of ArUco markers, perspective transformation, color calibration, and detection results. Since the image may be affected by environmental factors such as uneven light sources and background reflections, and we also embedded light-colored calibration blocks into ArUco markers, identification may fail. Before identifying the ArUco marker, the image is binarized and converted into a black and white image before identification. We continuously adjust the threshold for binarizing the image until the ArUco marker is successfully identified. After binarization, the image fails to be identified. The image that causes recognition failure is shown in Fig. 3(a), and the image obtained after adjusting the threshold is shown in Fig. 3(b).

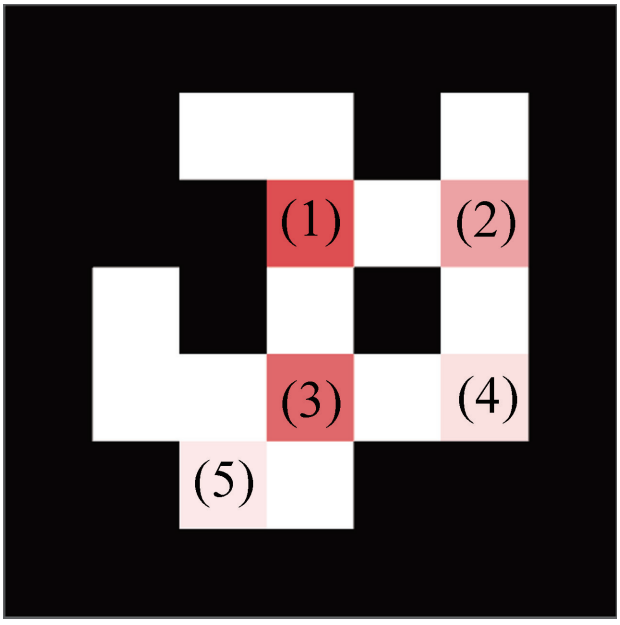

Fig. 2. (Color online) Proposed ArUco mark; (1) to (5) are calibration blocks.

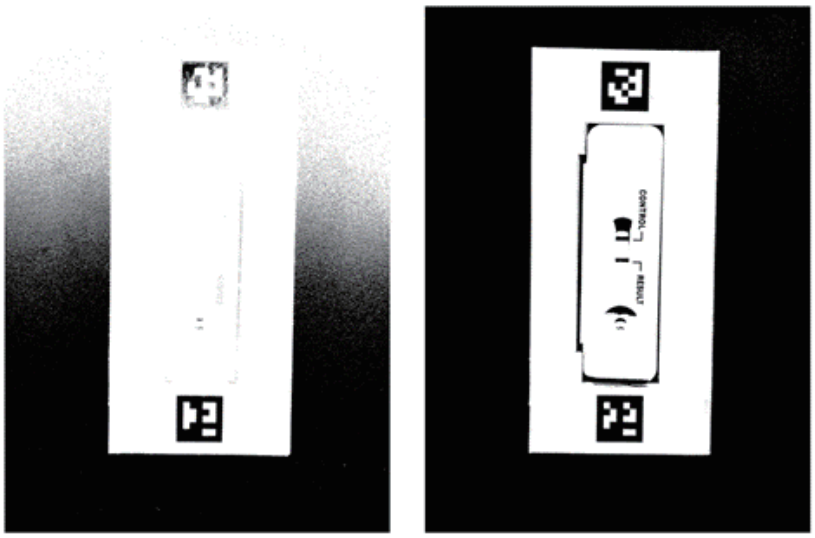

(a) (b)

Fig. 3. (a) Image that causes recognition failure and (b) image after adjustment of binarization threshold.

In this study, we used perspective transformation to correct any angular tilt caused by the user during photography. The coordinates of the ArUco marker on the colorimetric board are used to generate a mapping matrix. The mapping matrix is used to standardize the original image for detection by our method. The original image is shown in Fig. 4(a) and the converted image is shown in Fig. 4(b).

Before performing the color calibration and judging the results, the transmission-converted image is converted from the original color image to a grayscale image. Since the image is standardized through mapping conversion, the range of the captured region of interest (ROI) can be fixed. When processing the image, the calibration block in the ArUco marker is used as a standard to establish the range of the grayscale value presented by the test results and compare it with the grayscale value in the ROI. The final judgment is based on boundary detection, conversion to grayscale image statistics, and analysis of the full width at half-maximum (FWHM) position and size to avoid noise interference and determine the detection results and concentration. The grayscale image ROI and its internal grayscale value distribution are shown in Figs. 5(a)–5(c).

To confirm that the detection results and the HPY concentration can be identified by the method proposed in this study, a linearity experiment is conducted. Since the results of samples with different concentrations exhibit different colors, it is necessary to conduct experiments with multiple concentrations. In the experiment, the focus height is fixed and LED illumination in the simulated environment system is set to 700 Lux. The camera obscura is shown in Figs. 6(a) and 6(b).

Experiments were conducted using printed simulated tests and real rapid tests. The color lines of the simulated reagents used in the experiment are shown in Fig. 7.

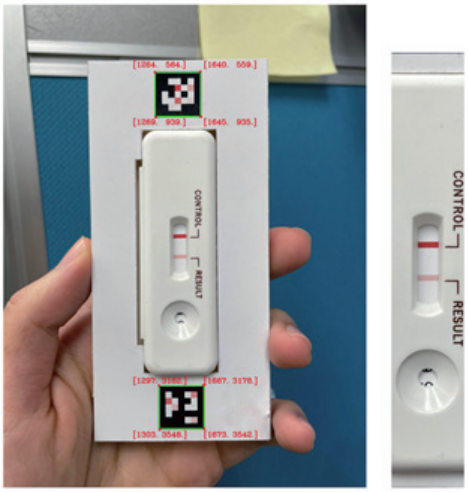

(a) (b)

Fig. 4. (Color online) (a) Original image and (b) image after perspective transformation.

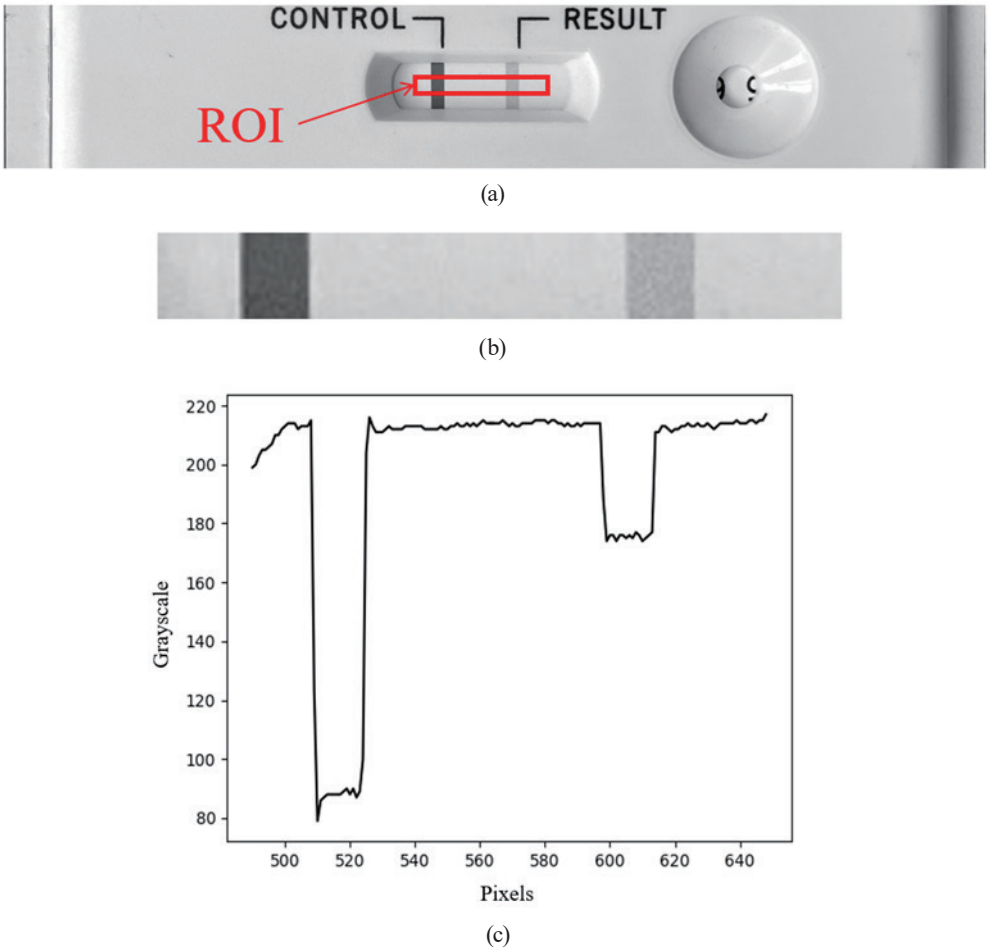

(a)

(b)

(c)

Fig. 5. (Color online) (a) ROI position of image, (b) ROI image, and (c) distribution of values within ROI.

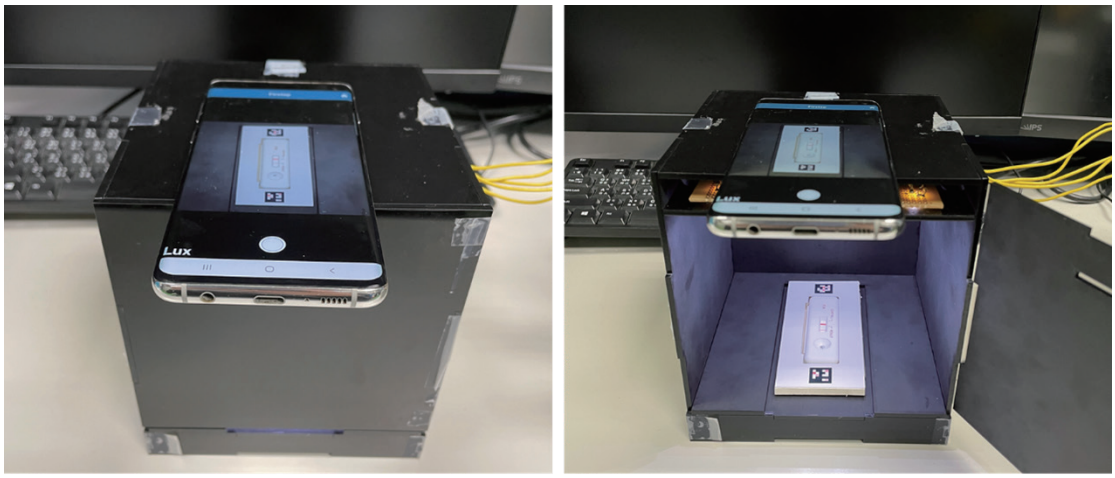

(a) (b)

Fig. 6. (Color online) (a) Camera obscura used in this study and (b) inside of the camera obscura.

Fig. 7. (Color online) Appearance of simulated test results.

Five colors indicating different sample concentrations were used for testing. For the real rapid test, 5000 CFU/mL was used in this study as the threshold for qualitative detection. Above this threshold, the result is positive; below it, it is negative. Using serial dilution, we prepared seven concentrations of test samples, namely, 7500, 6250, 5000, 3750, 2500, 1250, and 0 CFU/mL. We used four different smartphones in our experiments: iPhone 6 Plus, iPhone 12 PRO, Galaxy S10, and ROG Phone. Each smartphone analyzes each concentration five times.

3. Experiment Results

Each smartphone identified each sample concentration in the simulated tests five times, and the detection results were all correct. The gray scale values were read, and the actual gray scale values are statistically presented in Fig. 8.

There is obviously no overlap in Fig. 8. The coefficient of determination (R^2 value) is 0.9915 to 0.9995, which shows that each mobile phone has good linearity, indicating that the method proposed in this study can reduce the grayscale value error, thereby inferring the actual grayscale value.

Experiments were conducted using real rapid tests, and Fig. 9 shows the integrated results. It can be seen from Fig. 9 that the R^2 value is 0.977 to 0.9473. Even if there is a very low concentration of a real sample as the detection object, the method proposed in this study still has a considerable degree of detection consistency. It means that the method proposed in this study can effectively use the grayscale value range after color correction to determine the actual concentration.

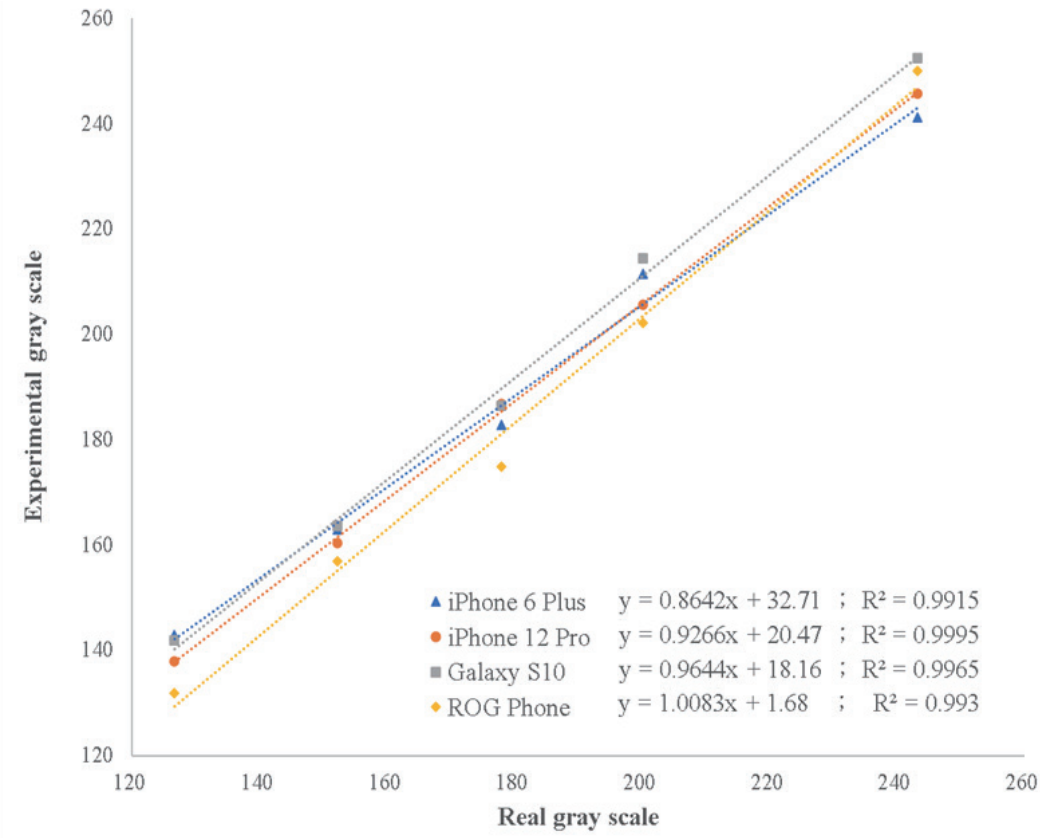

Fig. 8. (Color online) Actual and experimental grayscale value data chart of simulated rapid tests.

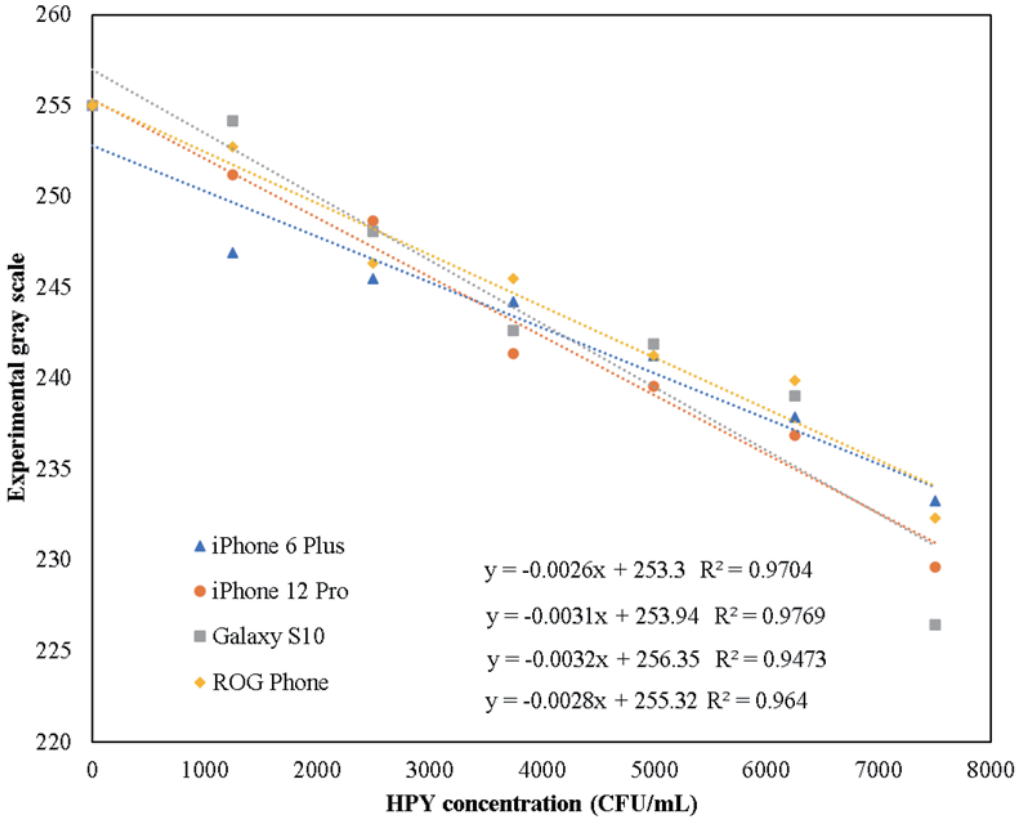

Fig. 9. (Color online) Real sample concentration and gray scale value data chart.

4. Conclusions

In the method proposed in this study, a mobile phone is used as an image capture device to evaluate the results of commercially available HPY rapid tests. To avoid misjudgments caused by environmental and device factors, we developed a colorimetric board to assist in image processing. The technology used on the colorimetric board includes the ArUco marker, color calibration, and perspective transformation. The coordinates of the ArUco marker can be used as the basis for perspective transformation to avoid coordinate positioning difficulties caused by different shooting angles. In this study, we embedded several calibration color blocks into the ArUco marker to reduce the space of the colorimetric board. Color calibration can not only suppress color deviations caused by different types of hardware, but also reduce the impact of different environmental factors on image shooting. The method proposed in this study has good linearity in experimental results. In the future, new detection algorithms can be added to accommodate other rapid-test products for detection, such as dengue fever, COVID-19, and luteinizing hormone.

Acknowledgments

This work was supported by the National Science and Technology Council, Taiwan, under grant no. NSTC 112-2221-E-006-192, to whom we express our deep gratitude.

References

1 M. Plummer, S. Franceschi, J. Vignat, D. Forman, and C. Martel: Int. J. Cancer **136** (2015) 487. https://doi.org/10.1002/ijc.28999
2 A. K. Azkur, M. Akdis, D. Azkur, M. Sokolowska, W. van de Veen, M. C. Bruggen, L. O'Mahony, Y. Gao, K. Nadeau, and C.A. Akdis: Allergy **75** (2020) 1564. https://doi.org//10.1111/all.14364
3 R. Rojanathanes, A. Sereemaspun, N. Pimpha, V. Buasorn, P. Ekawong, and V. Wiwanitkit: Taiwan. J. Obstet. Gynecol. **47** (2008) 296. https://doi.org/10.1016/S1028-4559(08)60127-8
4 D. Kutter: Clin. Chim. Acta **297** (2000) 297. https://doi.org/10.1016/S0009-8981(00)00255-2
5 K. Agha-Amiri, U. Peitz, D. Mainz, S. Kahl, A. Leodolter, and P. Malfertheiner: Z. Gastroenterol. **39** (2001) 555. https://doi.org/10.1055/s-2001-16629
6 T. Falsafi, N. Valizadeh, S. Sepehr, and M. Najafi: Clin. Vaccine Immunol. **12** (2005) 1094. https://doi.org/10.1128/CDLI.12.9.1094-1097.2005
7 E. G. Rey, D. O'Dell, S. Mehta, and D. Erickson: Anal. Chem. **89** (2017) 5095. https://doi.org/10.1021/acs.analchem.7b00638.
8 X. Tang and Y. Wang: 2011 Int. Conf. Image Analysis and Signal Process. (IEEE, 2011) 434. https://doi.org/10.1109/IASP.2011.6109078
9 S. Garrido-Jurado, R. Muñoz-Salinas, F. J. Madrid-Cuevas, and M. J. Marín-Jiménez: Pattern Recognit. **47** (2014) 2280. https://doi.org/10.1016/j.patcog.2014.01.005
10 Y. Do: 2013 10th IEEE Int. Conf. Control and Automation (IEEE, 2013) 418. https://doi.org/10.1109/ICCA.2013.6565144
11 N. Stamatopoulos, B. Gatos, I. Pratikakis, and S. J. Perantonis: IEEE Trans. Image Process. **20** (2011) 910. https://doi.org/10.1109/TIP.2010.2080280.
12 Y. C. Chang and J. F. Reid: IEEE Trans. Image Process. **5** (1996) 1414. https://doi.org/10.1109/83.536890
13 P. D. M. Fernández, F. A. G. Peña, T. I. Ren, and J. J. G. Leandro: Image Vision Comput. **81** (2019) 15. https://doi.org/10.1016/j.imavis.2018.11.001
14 Y. Cao, Y. Liu, F. Li, S. Guo, Y. Shui, H. Xue, and L. Wang: Microchem. J. **150** (2019) 104176. https://doi.org/10.1016/j.microc.2019.104176
15 N. Phadungcharoena, P. Patrojanasophon, P. Opanasopit, T. Ngawhirunpat, A. Chinsriwongkul, and T. Rojanarata: Int. J. Pharm. **558** (2019) 120. https://doi.org/10.1016/j.ijpharm.2018.12.078.

About the Authors

Yu-Lin Wu received his M.S. degree in computer science and information engineering from National Changhua University of Education in 2017. He is a doctoral student in the Department of Engineering Science at National Cheng Kung University, Tainan, Taiwan. (n98091039@gs.ncku.edu.tw)

Wei-Chien Weng received his M.S. degree in engineering science from National Cheng Kung University of Education in 2017. His main research interests include microstructure design, biomedical applications, and biomedical equipment development. He is a doctoral student in the Department of Engineering Science at National Cheng Kung University, Tainan, Taiwan. (lu4a04@gmail.com / n98104028@gs.ncku.edu.tw)

Yi-Hsuan Chen received her M.S. degree in engineering science from National Cheng Kung University of Education in 2022. Her main research interests include microstructure design, biomedical applications, and semiconductor processes. She is an engineer at TSMC, Taiwan. (nckuyuclin@gmail.com)

Yu-Cheng Lin received his Ph.D. degree in electrical engineering from the University of Illinois at Chicago in 1996. He is a Distinguished Professor in the Department of Engineering Science at National Cheng Kung University, Tainan, Taiwan. His main research interests include bio-MEMS, microfluidic systems, and nanotechnology in biomedical applications. He is currently an associate editor of IEEE Sensors Journal and an editorial advisory board member of Sensors and Actuators A: Physical. He was the Vice President of Conferences of IEEE Sensors Council for 2014–2017. He was elected as a Fellow of the Royal Society of Chemistry in 2008, a Fellow of the International Society for Optics and Photonics (SPIE) in 2012, and a Fellow of the Institution of Engineering and Technology (IET) in 2013. (yuclin@mail.ncku.edu.tw)